Bayesian, Maneuver-Based, Long-Term Trajectory Prediction and Criticality Assessment for Driver Assistance Systems

Matthias Schreier, Volker Willert, Jürgen Adamy

Abstract— **We propose a Bayesian trajectory prediction and criticality assessment system that allows to reason about imminent collisions of a vehicle several seconds in advance. We first infer a distribution of high-level, abstract driving maneuvers such as lane changes, turns, road followings, etc. of all vehicles within the driving scene by modeling the domain in a Bayesian network with both causal and diagnostic evidences. This is followed by maneuver-based, long-term trajectory predictions, which themselves contain random components due to the immanent uncertainty of how drivers execute specific maneuvers. Taking all uncertain predictions of all maneuvers of every vehicle into account, the probability of the ego vehicle colliding at least once within a time span is evaluated via Monte-Carlo simulations and given as a function of the prediction horizon. This serves as the basis for calculating a novel criticality measure, the Time-To-Critical-Collision-Probability (TTCCP) – a generalization of the common Time-To-Collision (TTC) in arbitrary, uncertain, multi-object driving environments and valid for longer prediction horizons. The system is applicable from highly-structured to completely non-structured environments and additionally allows the prediction of vehicles not behaving according to a specific maneuver class.**

I. INTRODUCTION AND MOTIVATION

Future Advanced Driver Assistance Systems (ADAS) must not just react to the actual state of the environment, but anticipate the future evolution of the traffic scene to perform correct decisions, warnings and interventions. Whereas this evolution can reasonably be predicted for a short time (typically less than a second) by just considering physical quantities such as estimated vehicles' velocities or yaw rates, the evolution over several seconds is much stronger influenced by the intentions, motivations and goals of all traffic participants within the specific driving environment. This raises the complexity for longer-term predictions considerably. Two major challenges exist in the design of long-term trajectory prediction and criticality assessment algorithms for active collision avoidance and warning systems. First, it is neither optimal to determine just a single future trajectory for each vehicle nor is it reasonable to predict every physically possible trajectory. In the first case, the one and only future hypothesis will most certainly not occur whereas human drivers take different scene evolutions into account. In the second case, false warnings will be generated. For example, the reachable sets of two oncoming vehicles on different lanes will overlap after a very short prediction horizon although this standard situation is usually uncritical.

M. Schreier, V. Willert and J. Adamy are with the Institute of Automatic Control and Mechatronics, Control Methods and Robotics Lab, TU Darmstadt, Landgraf-Georg-Str. 4, 64283 Darmstadt, Germany {schreier,vwillert,jadamy}@rtr.tu-darmstadt.de

The second less considered challenge is that the further one tries to predict into the future, the more assumptions have to be made, which tempts to model the average, sensible driver in a given traffic situation. As an extreme example, the prediction could be based upon the assumption that every driver obeys the traffic rules or follows the road flawlessly. Although these assumptions are reasonable for microscopic traffic simulations, they are not appropriate for active safety systems, because especially actions that do not match the traffic rules and contradict with the standard situation evolution might become dangerous. Thus, all prediction methods that are solely based upon the average driver are not suitable for an emergency situation ADAS as exactly these situations are excluded by the prediction assumptions beforehand and therefore cannot be predicted at all.

Consequently, the system must i) be sensitive to exceptional, rarely happening situations, ii) should not only consider physical quantities but also information about the drivers' intentions and the driving environment and iii) take into account only a reasonable subset of possible future scene evolutions.

As the drivers' intentions manifest in form of high-level driving maneuvers, it seems beneficial to first infer these more abstract hidden states. Our approach then connects the abstract, qualitative maneuver detection with the quantitative trajectory prediction domain with the ultimate goal to calculate a criticality measure suitable for arbitrary, uncertain driving environments for longer prediction time spans – the so-called Time-To-Critical-Collision-Probability (TTCCP).

II. RELATED WORK

Long-term trajectory prediction methods can be classified into methods of pattern recognition in motion pattern databases [1], [2] and approaches fusing dynamic motion models with behavior and/or environment descriptions [3]–[6]. Besides the problem of generating, saving and fitting large motion pattern data records, the first group has the immanent disadvantage that only trajectories included in the database can be predicted. This makes them unsuitable for criticality assessment due to their inability to predict abnormal situations. Some representatives of the second group, which consider uncertainty and additionally include a criticality assessment part, are explained in the following.

The approaches of [4], [5] perform probabilistic trajectory predictions by employing path-planning algorithms from the viewpoint of each traffic participant to generate distributions over future motions of all vehicles. Different combinations of future system inputs are considered via Monte-Carlo

simulations while the stochastic inputs are restricted to specific, typical human driving behaviors and actions such as lane changes or overtaking – a similarity to our approach. They are, however, the result of goal functions, which model behaviors. No explicit maneuver detections are performed. The result is a probability of collision for the complete traffic scene as well as a so-called danger level display for each road position at each future time.

In [3], stochastic reachable sets of all other (interacting) traffic participants are determined assuming that they follow specific paths along a known road network with a certain accuracy. The ego vehicle's future path is considered known as the system is designed for autonomous vehicles with a known planned future trajectory and not for ADAS. The longitudinal dynamic motion models of other vehicles along their paths are abstracted into discrete Markov chains, the lateral positions are described by predefined, fixed distributions. The future actions "go straight" and "turn" are considered for the other vehicles. As their motions are constrained along road geometries and speed limits, an unintentional leaving of the road cannot be detected.

The approach of [6] allows longer-term criticality assessment in structured highway environments and focuses on the interaction of traffic participants. By updating a hand-designed prior intention distribution with results of the corresponding, fictive collision probabilities stemming from the execution of each intention, so-called interaction-aware maneuver probabilities are estimated. They are based on the postulation that drivers do not perform maneuvers with high collision risks as long as safer options are possible. This assumption, however, inevitably prevents the detection of specific dangerous situations such as colliding with a slower vehicle on the same lane, if there is still a free adjacent lane for a possible lane change. Our approach, in contrast, predicts maneuvers only in case physically measurable evidences indicate a maneuver.

Besides explicit trajectory prediction methods, numerous approaches reason about the future traffic scene on a more abstract level. The mathematical tools comprise probabilistic state machines [7], static Bayesian networks [8], general dynamic Bayesian networks [9], Hidden Markov Models (HMM's) [10], Dempster-Shafer theory [11], fuzzy theory [7] or specific classifiers [12]. Our approach connects a novel Bayesian network-based, qualitative maneuver detection approach with the quantitative, uncertain trajectory prediction domain to generate long-term predictions – a similar two-step approach with layered HMM's for maneuver detection can be found in [13].

In the subsequent situation criticality assessment, Time-To-X (TTX) metrics such as the Time-To-Collision (TTC) are common [14]. A recent extension [15] additionally considers uncertainty by calculating a probability distribution over TTC's via the Unscented Transform. In contrast to our approach, however, only uncertain state estimates are considered and not additional uncertainties in the drivers' behaviors.

III. SYSTEM OVERVIEW

The system is subdivided into three main parts: The maneuver detection, the prediction and the criticality assessment part as shown in Fig. 1.

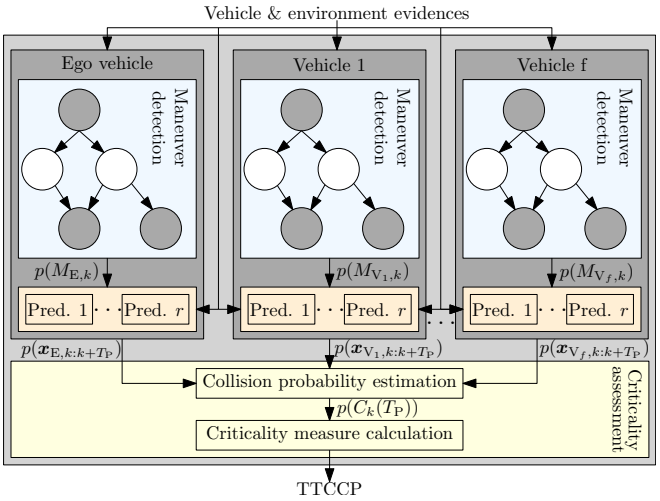

Fig. 1. System overview.

In the maneuver detection part (blue), every vehicle's actual driving maneuvers are estimated via Bayesian inference. For this purpose, a Bayesian network is modeled and fed with measured vehicle and environment evidences. The inference result is a probability mass function (pmf) $p(M_{\mathrm{E},k})$ of the discrete maneuver random variable $M_{\mathrm{E},k}$ for the ego vehicle at each time step k as well as for the $i = 1, \ldots, f$ additional vehicles $V_{i,k}$ within the observed traffic scene $p(M_{\mathrm{V}_i,k})$.

In the prediction part (orange), maneuver-specific prediction models are employed to predict the configuration $\boldsymbol{x} = (x, y, \psi)^T$ of each vehicle forward in time within a common global coordinate system. The individual $j = 1, \ldots, r$ prediction models are adapted to the actual driving environment and uncertainties in the drivers' future maneuver realizations are taken into account by introducing uncertainties within these models. Therefore, even if we knew a driver is performing a specific maneuver for sure, the prediction model would nevertheless generate many possible trajectory realizations of this maneuver. The result of the prediction part is a joint probability distribution function (pdf) $p(\boldsymbol{x}_{k:k+T_\mathrm{P}})$ of future configurations over the $T_\mathrm{P} \in \mathbb{N}$ prediction time steps for each vehicle.[1]

In the criticality assessment part (yellow), these individual joint distributions are used to estimate the collision probability $p(C_k(T_\mathrm{P}))$ of the event that the ego vehicle collides with at least one other vehicle at least once within the prediction horizon $[k, k + T_\mathrm{P}]$ via Monte-Carlo simulation. Subsequently, the TTCCP criticality measure is calculated as the necessary prediction time until the probability of this collision event exceeds a certain value. It is therefore a time measure analogous to TTC, which, however, takes all

[1]For shorter notation, the sequence $k, k+1, \ldots, k+T_\mathrm{P}$ is written as $k : k + T_\mathrm{P}$.

possible future traffic scene evolutions into account. In the following, the three parts are explained in more detail.

A. MANEUVER DETECTION

The Bayesian network for maneuver detection is modeled with the application criticality assessment in mind and therefore needs to allow the detection of exceptional, non-standard situations. This can hardly be accomplished by modeling a single, complex network that takes interactions between all traffic participants into account. This approach would inevitably lead to the design of average traffic situations, thus preventing the detection and subsequent prediction of rare events.[2] In contrast, we instantiate a separate network for every vehicle that primarily obtains evidences independent from other traffic participants. The last statement can be justified by thinking about, for example, adding the evidence that a neighboring vehicle occupies the ego vehicle's adjacent lane such as done in [8]. Then this evidence could only be reasonably included into the network in a way that it lowers the probability of an impending lane change for the ego vehicle due to the occupied adjacent lane. If weighted too strongly, this evidence would prevent the prediction of a collision if the ego vehicle indeed performs the unlikely lane change and is therefore intentionally not included in our network. As a result of these considerations, our network is designed under the implicit premise of drivers overlooking each other, at least, unless physical evidence contradicts this premise. An example for this is a vehicle already braking strongly in front of an obstacle. In this situation, the prediction of the timely stop prevents false warnings and is therefore incorporated.

The developed network is shown in Fig. 2. It consists of 8 binary (true and false) maneuver nodes within the maneuver layer (blue), 6 helper nodes (yellow) and 16 evidence nodes (shaded) subsumed in Table I. All naturally continuous random variables such as velocities are discretized by dividing their values into several reasonable intervals. Thus, the complete network is discrete. We do not use either causal (predictive – from cause to effect as in [8]) or diagnostic (evidential – from effect to cause as in [16]) reasoning, but both by embedding the hidden maneuver node layer in-between the observable causal and diagnostic evidence node layers, which additionally allows intercausal reasoning. The main consideration in the network design process is that the causal evidence layer models requirements for specific maneuvers to happen. The existence of a neighboring lane, for example, is a necessity for a lane change maneuver or the time until a turning is reached influences the probability of an oncoming turn maneuver. The diagnostic evidence layer, in contrast, models the maneuvers' consequences (symptoms) in form of measurable physical motion states. We use longitudinal and lateral vehicle acceleration $a_{\mathrm{R,lon/lat}}$, lateral velocity $v_{\mathrm{R,lat}}$ and yaw angle ψ_{R} within a lane-fixed coordinate system as diagnostic evidences. These are partly not directly connected with the maneuver layer, but via helper nodes $\mathrm{LAT_{l/r}}$ and LON for lateral and longitudinal motion, respectively. This simplifies the parametrization of the corresponding Conditional Probability Tables (CPT's).

[2]This could, however, be a reasonable approach for other applications such as cognitive, autonomous vehicles that need the understanding of the standard future traffic scene evolution for adequate decision making.

TABLE I

RANDOM VARIABLES OF TYPE CAUSAL EVIDENCE (CE), DIAGNOSTIC EVIDENCE (DE), HELPER NODE (HN) AND MANEUVER NODE (MN).

Variable	Type	Explanation
$\mathrm{LE_{l/r/a}}$	CE	Lane existence left/right/actual
$\mathrm{TLC_{l/r}}$	CE	Time to line crossing left/right
$\mathrm{TTU_{l/r}}$	CE	Time to turning left/right
$\mathrm{TE_{l/r}}$	CE	Turning existence left/right
v_{rel}	CE	Relative velocity to front object
$\mathrm{OE_{fro}}$	CE	Front object existence
$\mathrm{TO_{fro}}$	CE	Time to front object
ψ_{R}	DE	Yaw angle to road tangent
$a_{\mathrm{R,lat}}$	DE	Lateral acceleration perpendicular to road tangent
$v_{\mathrm{R,lat}}$	DE	Lateral velocity perpendicular to road tangent
$a_{\mathrm{R,lon}}$	DE	Longitudinal acceleration along road tangent
$\mathrm{TR_{l/lon/r}}$	HN	Trash class helper left/longitudinal/right
$\mathrm{LAT_{l/r}}$	HN	Lateral motion left/right
LON	HN	Longitudinal motion
$\mathrm{LC_{l/r}}$	MN	Lane change to the left/right
$\mathrm{TU_{l/r}}$	MN	Turn to the left/right
TR	MN	Trash maneuver class (no maneuver)
FV	MN	Follow vehicle
FR	MN	Follow road
TB	MN	Target brake

The combination of causal and diagnostic evidences allows explaining away. If, for example, the observed states of the diagnostic nodes are indistinguishable consequences of either a lane change or a turn maneuver, then the additional causal knowledge of a non-existing turning automatically raises the probability that the observed diagnostic evidence stems from a lane change. Moreover, the design approach allows to integrate a trash maneuver class TR for modeling all motions not belonging to a specific maneuver class, e.g. irrational movements of a drunken driver, by explaining away all contradictory evidence to the trash maneuver class via the helper nodes $\mathrm{TR_{l/lon/r}}$. These are connected to TR in a noisy-or manner. The trash maneuver class also gets a high probability if all other maneuver requirements are missing, e.g. no lane or turning information is available such as in completely unstructured environments like parking zones or dirt tracks.

In every time step k, the network is updated with all available evidences. Then, the individual maneuver nodes are normalized so that they form a single, valid, discrete maneuver random variable M with the 8 maneuver states and corresponding pmf $p(M)$.

B. TRAJECTORY PREDICTION

For each maneuver, a prediction model is set up. In Fig. 3, the mean predicted trajectories of each maneuver class are qualitatively visualized. Each model is adapted to the actual traffic scene situation by taking vehicle and environment evidences into account such as lane width or the distance to a stopping point. They additionally contain random components to model different driving styles and are

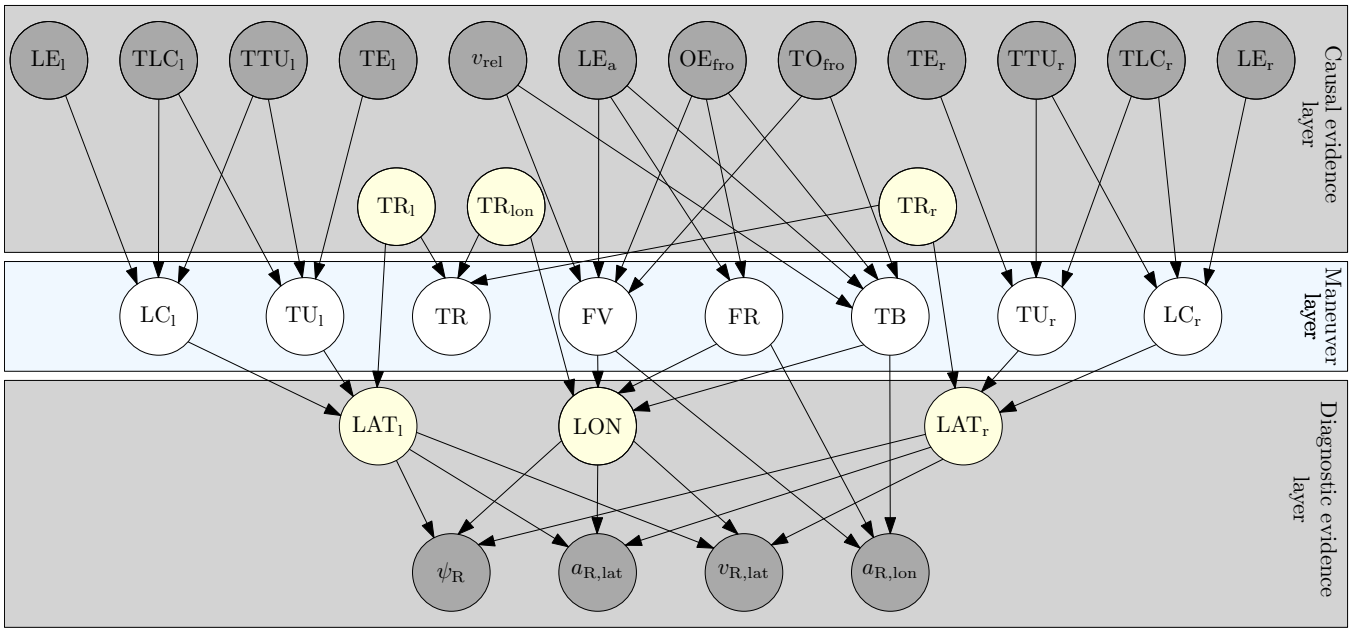

Fig. 2. Bayesian network for maneuver detection instantiated for each vehicle within the traffic scene at each time step k. Hidden maneuver nodes (blue) are inferred via Bayesian inference given causal and diagnostic evidence nodes (shaded). Helper nodes (yellow) are used to facilitate parametrization. Abbreviations are explained in Table I.

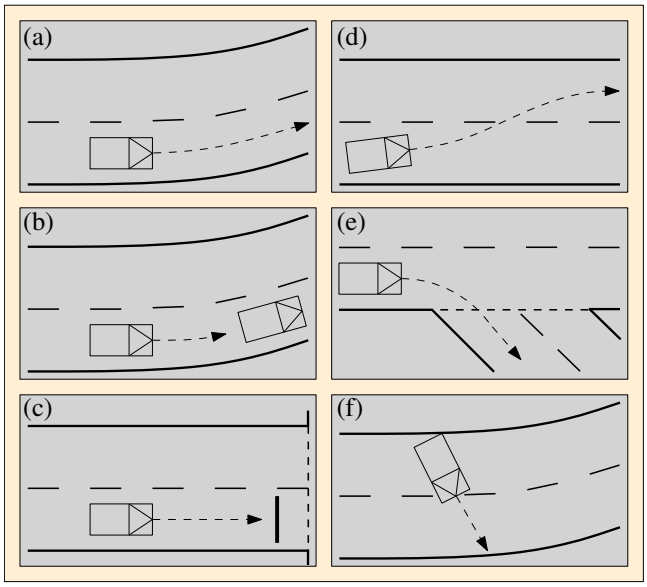

Fig. 3. Maneuver-based prediction models. Follow road (a), Follow vehicle (b), Target brake (c), Lane change (d), Turn (e), Trash maneuver class (f). Dashed trajectories correspond to mean predicted trajectories.

shortly explained in prose in the following.[3]

- Follow road: The model predicts the vehicle's longitudinal position along the road according to a (nearly) constant acceleration model in which the acceleration is treated as a random variable with normal distribution around the actual acceleration and linearly growing variance over the prediction horizon to model the rising uncertainty in the driver's acceleration profile. Negative velocities are suppressed. The vehicle's lateral position along the road follows a normal distribution around the actual lateral position and a standard deviation designed such that a vehicle driving in the middle of the road is completely inside the lane corresponds to the three sigma interval. The yaw angle along the road is likewise following a normal distribution with zero mean and small allowed deviations as the vehicle's orientation is supposed to nearly correspond to the road orientation in a follow road maneuver.
- Follow vehicle: The model is based on the assumption that the driver reacts to another vehicle in front and accelerates in a way that an adequate mean time gap of $2\,\mathrm{s}$ occurs. The acceleration assumes moderate reaction (acceleration bounds between $-3.5\,\frac{\mathrm{m}}{\mathrm{s}^2}$ and $2.5\,\frac{\mathrm{m}}{\mathrm{s}^2}$) of the driver similar to adaptive cruise control systems and does therefore not predict abrupt braking maneuvers. The model can predict collisions if the driver reacts to a vehicle in front too slightly as well as also suppress false warnings that would occur if a driver moderately reacts to vehicles further away, in which a pure follow road maneuver would already predict a collision. Lateral and yaw angle deviations are modeled analogous to the follow road maneuver.
- Target brake: The model predicts under the assumption that the vehicle stops in front of a braking target such as an obstacle, another vehicle or a stop line. The predicted acceleration equals the necessary constant acceleration for the vehicle to stop in a specified distance to the

[3]Due to space limitations, the complete mathematical description of the maneuver prediction models is omitted as not considered crucial for understanding the concept.

braking target.[4] This distance is treated as normally distributed around $1\,\mathrm{m}$ with standard deviation designed in a way that a vehicle stopping directly in front of the braking target with no safety margin corresponds to the three sigma interval.

- Lane change: The model predicts lane changes under the assumption that both lanes have the same width and the maneuver started nearly in the middle of the lane. The trajectory is supposed to follow a sine half-cycle in road coordinates, which is scaled based on the expected distance along the road coordinate until the maneuver is finished. This distance is calculated by aligning the tangent of the sine shape with the vehicle's actual orientation at each time step. The uncertainty within the predicted lateral displacement and yaw angle is modeled by considering the lateral maneuver origin around the middle of the lane from which the maneuver started as normally distributed. The longitudinal acceleration along the road coordinate equals the follow road model. As soon as the end of the sine half-cycle is reached, the model obeys the follow road model for the remaining prediction horizon.
- Turn: The model predicts turns by partitioning the maneuver into three segments. Before the vehicle leaves the initial road, the turning itself and the remaining prediction on the destination road after the turning. The prediction in the first segment follows a straight line along the initial road with a constant acceleration model with predicted acceleration calculated as the mean, necessary (negative) acceleration required in a way that a maximal velocity is not exceeded at the start of the turn. This maximal velocity is itself determined so that the driver is only exposed to a maximal centripetal acceleration during the second segment, the actual turning phase. Here, the transition between the two roads is modeled as a circular arc. The arc's center lies on the angle bisector between the two road tangents, the radius is adapted according to the roads' geometry so that initial and destination roads' tangents are also tangents of the circle. The third segment on the destination road is again a straight line. The longitudinal motion in segment two and three is realized via a constant velocity model, lateral positions on the initial and destination road are considered random variables following a normal distribution to model different turn executions as every driver cuts the corner differently.
- Trash maneuver class: The model predicts the motion according to a (nearly) Constant Turn Rate and Acceleration model (CTRA), i.e. purely based on physical states with no environment knowledge required.

Every maneuver prediction model generates, in a very general sense, a joint pdf over the prediction horizon $p(\boldsymbol{x}_{k:k+T_\mathrm{P}}|M_{j,k})$ with configuration $\boldsymbol{x} = (x, y, \psi)^T$ for all $j = 1, \ldots, r$ maneuvers for each vehicle. By marginalizing out the maneuver states from the combined pdf $p(\boldsymbol{x}_{\mathrm{E},k:k+T_\mathrm{P}}, M_k)$ with the help of $p(M_{\mathrm{E},k})$ and $p(M_{\mathrm{V}_i,k})$ from the Bayesian network inference result of section III-A, we reach

$$\begin{aligned} p(\boldsymbol{x}_{\mathrm{E},k:k+T_\mathrm{P}}) &= \sum_{j=1}^{r} p(\boldsymbol{x}_{\mathrm{E},k:k+T_\mathrm{P}}|M_{\mathrm{E},k}=j)p(M_{\mathrm{E},k}=j), \\ p(\boldsymbol{x}_{\mathrm{V}_i,k:k+T_\mathrm{P}}) &= \sum_{j=1}^{r} p(\boldsymbol{x}_{\mathrm{V}_i,k:k+T_\mathrm{P}}|M_{\mathrm{V}_i,k}=j)p(M_{\mathrm{V}_i,k}=j), \end{aligned} \tag{1}$$

for the ego vehicle and the other $i = 1, \ldots, f$ vehicles, respectively. These densities are used for criticality assessment in the following.

C. CRITICALITY ASSESSMENT

In [17], a general formula for probabilistic collision checking is presented which, however, only holds for calculating the collision probability of two uncertain, extended objects at a specific point in time. Adapted to our case, the probability of the ego vehicle colliding exactly with vehicle V_i at a specific, common point in time is given by[5] [17]

$$p(C) = \int_{\boldsymbol{x}_{\mathrm{V}_i}} \int_{\boldsymbol{x}_\mathrm{E}} I_{C1}(\boldsymbol{x}_\mathrm{E}, \boldsymbol{x}_{\mathrm{V}_i}) p(\boldsymbol{x}_\mathrm{E}, \boldsymbol{x}_{\mathrm{V}_i}) \mathrm{d}\boldsymbol{x}_\mathrm{E} \mathrm{d}\boldsymbol{x}_{\mathrm{V}_i} \tag{2}$$

with joint density over the uncertain configurations of both vehicles $p(\boldsymbol{x}_\mathrm{E}, \boldsymbol{x}_{\mathrm{V}_i})$ and collision indicator function

$$I_{C1}(\boldsymbol{x}_\mathrm{E}, \boldsymbol{x}_{\mathrm{V}_i}) = \begin{cases} 1, & \mathcal{S}(\boldsymbol{x}_\mathrm{E}) \bigcap \mathcal{S}(\boldsymbol{x}_{\mathrm{V}_i}) \neq \emptyset, \\ 0, & \text{else.} \end{cases} \tag{3}$$

Here, $\mathcal{S}(\boldsymbol{x}_\mathrm{E})$ and $\mathcal{S}(\boldsymbol{x}_{\mathrm{V}_i})$ refer to the set of points in space that are occupied by the ego and obstacle vehicle when their configurations are given by $\boldsymbol{x}_\mathrm{E}$ and $\boldsymbol{x}_{\mathrm{V}_i}$, respectively. For criticality assessment over a future time span, i.e. the calculation of the probability of the event $C_{\mathrm{V}_i,k}(T_\mathrm{P})$: *The ego vehicle collides with vehicle V_i at least once within the prediction horizon* $[k, k+T_P]$, evaluated at time step k, the formula has to be generalized as follows:

$$\begin{aligned} p(C_{\mathrm{V}_i,k}(T_\mathrm{P})) = &\int_{\boldsymbol{x}_{\mathrm{V}_i,k+T_\mathrm{P}}} \int_{\boldsymbol{x}_{\mathrm{E},k+T_\mathrm{P}}} \cdots \int_{\boldsymbol{x}_{\mathrm{V}_i,k}} \int_{\boldsymbol{x}_{\mathrm{E},k}} \\ &I_C(\boldsymbol{x}_{\mathrm{E},k:k+T_\mathrm{P}}, \boldsymbol{x}_{\mathrm{V}_i,k:k+T_\mathrm{P}}) p(\boldsymbol{x}_{\mathrm{E},k:k+T_\mathrm{P}}, \boldsymbol{x}_{\mathrm{V}_i,k:k+T_\mathrm{P}}) \\ &\mathrm{d}\boldsymbol{x}_{\mathrm{E},k} \mathrm{d}\boldsymbol{x}_{\mathrm{V}_i,k} \ldots \mathrm{d}\boldsymbol{x}_{\mathrm{E},k+T_\mathrm{P}} \mathrm{d}\boldsymbol{x}_{\mathrm{V}_i,k+T_\mathrm{P}} \end{aligned} \tag{4}$$

with new collision indicator function

$$I_C(\boldsymbol{x}_{\mathrm{E},k:k+T_\mathrm{P}}, \boldsymbol{x}_{\mathrm{V}_i,k:k+T_\mathrm{P}}) = \begin{cases} 1, & \exists m \in [k, k+T_\mathrm{P}] : \\ & \mathcal{S}(\boldsymbol{x}_{\mathrm{E},m}) \bigcap \mathcal{S}(\boldsymbol{x}_{\mathrm{V}_i,m}) \\ & \neq \emptyset, \\ 0, & \text{else.} \end{cases} \tag{5}$$

Therefore, an integration over the volume of the joint density over both vehicles and all future time steps, at which the

[4] If this lies below the minimal acceleration of $-8\,\frac{\mathrm{m}}{\mathrm{s}^2}$, this value is used instead.

[5] The short notation $\int_{\boldsymbol{x}}(.)\mathrm{d}\boldsymbol{x}$ means integration over the whole range of $\boldsymbol{x}$, e.g. if $\boldsymbol{x} = (x_1, \ldots, x_n)^T \in \mathbb{R}^n$, then $\int_{\boldsymbol{x}}(.)\mathrm{d}\boldsymbol{x} = \int_{\mathbb{R}^n}(.)\mathrm{d}\boldsymbol{x} = \int_{-\infty}^{\infty} \cdots \int_{-\infty}^{\infty}(.)\mathrm{d}x_1 \ldots \mathrm{d}x_n$.

collision condition is fulfilled, is necessary.[6] We further consider the trajectories of all vehicles as independent[7], therefore the joint density in (4) reduces to

$$p(\boldsymbol{x}_{\mathrm{E},k:k+T_\mathrm{P}}, \boldsymbol{x}_{\mathrm{V}_i,k:k+T_\mathrm{P}}) = p(\boldsymbol{x}_{\mathrm{E},k:k+T_\mathrm{P}})p(\boldsymbol{x}_{\mathrm{V}_i,k:k+T_\mathrm{P}}) \quad (6)$$

with the pdf's on the right hand side given by (1). For all f obstacle vehicles, the probability of the combined event $C_k(T_\mathrm{P})$: *The ego vehicle collides with at least one vehicle at least once within the prediction horizon* $[k, k+T_P]$, evaluated at time step k, can now be calculated as

$$\begin{aligned} p(C_k(T_\mathrm{P})) &= p\left(\bigcup_{i=1}^{f} C_{\mathrm{V}_i,k}(T_\mathrm{P})\right) = p\left(\neg \bigcap_{i=1}^{f} \neg C_{\mathrm{V}_i,k}(T_\mathrm{P})\right) \\ &= 1 - p\left(\bigcap_{i=1}^{f} \neg C_{\mathrm{V}_i,k}(T_\mathrm{P})\right) = 1 - \prod_{i=1}^{f} \left(1 - p(C_{\mathrm{V}_i,k}(T_\mathrm{P}))\right), \end{aligned} \quad (7)$$

in which the last step follows from the stochastic independence assumption of the individual (not mutually exclusive) collision events. Considering (7) as a function of T_P, i.e. the length of the prediction horizon (number of prediction time steps), then the criticality measure TTCCP as the time until the combined collision probability $p(C_k(T_\mathrm{P}))$ exceeds a Critical Collision Probability (CCP) can be calculated as

$$\mathrm{TTCCP} = \min(T_\mathrm{P} | p(C_k(T_\mathrm{P})) > \mathrm{CCP}) \cdot T, \quad (8)$$

with prediction sampling time T. This can be seen as a generalization for the criticality measure TTC in uncertain driving environments. In a practical implementation, (4) is solved via Monte Carlo simulation, so that the expectation of the indicator function, i.e. the collision probability, can be estimated by

$$p(C_{\mathrm{V}_i,k}(T_\mathrm{P})) = \mathbb{E}(I_C) \approx \frac{1}{N} \sum_{i=1}^{N} I_C(\tilde{\boldsymbol{x}}_i), \quad (9)$$

in which $\tilde{\boldsymbol{x}}_i$ is one out of N independent and identically distributed drawn samples from the joint density $p(\boldsymbol{x}_{\mathrm{E},k:k+T_\mathrm{P}}, \boldsymbol{x}_{\mathrm{V}_i,k:k+T_\mathrm{P}})$ and the unbiased estimate converging almost surely to the true collision probability by the strong law of large numbers with convergence rate of order $\mathcal{O}(\frac{1}{\sqrt{N}})$. Each sample therefore corresponds to two complete predicted trajectories. Although, following (6), the trajectories of the vehicles can be drawn independently of each other, the specification of the Monte Carlo estimate in this more general form is advantageous, as it then becomes directly obvious that only a single summation over simultaneously drawn samples from both individual distributions $p(\boldsymbol{x}_{\mathrm{E},k:k+T_\mathrm{P}})$ and $p(\boldsymbol{x}_{\mathrm{V}_i,k:k+T_\mathrm{P}})$ is required, which is further elaborated and justified in [17]. This way, much less samples are needed to obtain the same estimation error in opposition to a naive double summation over individual trajectory samples.

IV. IMPLEMENTATION AND RESULTS

The complete system has been implemented in C++ and coupled with the simulation environment IPG Carmaker. For Bayesian network inference, we employ the junction tree algorithm.The system has been parameterized by hand by constructing manifold driving situations within the simulation environment. In the following, two exemplary driving situations are shown to illustrate the approach.[8] In the first example shown in Fig. 4(a,b,c), the ego vehicle approaches another vehicle (blue) driving in the same direction on the same lane, decelerates rapidly ($t \approx 4\,\mathrm{s}$) to successfully prevent a collision and subsequently performs a lane change ($t \approx 6\,\mathrm{s}$) to the left to overtake. On the adjacent lane, however, an oncoming vehicle (red) approaches with which the ego vehicle finally collides at $t = 7.6\,\mathrm{s}$. The maneuver estimation (Fig. 4d) clearly shows the individual driving maneuvers (in successive order: follow vehicle, target brake, lane change to the left, follow road) for the ego vehicle – the other two vehicles just follow the road with constant velocity. Fig. 4e illustrates the scene from a bird's eye view and visualizes predicted trajectory samples of our approach with corresponding combined collision probabilities over the respective future $3\,\mathrm{s}$ time horizons in contrast to standard, deterministic CTRA (Fig. 4f) and CV (Fig. 4g) models.[9] The ego vehicle and the two other vehicles' centered rear points are shown with blue and green circles, respectively. It becomes clearly visible that the deterministic predictions that do not consider environment knowledge cannot reasonably perform longer-term predictions. The derived criticality measures (TTC (CV/CTRA)) and TTCCP are shown in Fig. 4h. The TTC calculated via a CV model generates false positive criticality values at $t \approx 4\,\mathrm{s}$ as it does not consider the deceleration of the ego vehicle before performing the lane change, the TTC with a CTRA model as well as our approach do not show this undesirable result. Our approach, at this stage, mainly predicts via target brake and – to a lesser extend – via a follow vehicle model. Additionally, we see that the true collision can be detected first by our method due to mainly predicting via a lane change model during the lane change. Note that the first two TTC (CTRA) values stem

[6]Note that it is incorrect to combine the collision probabilities calculated via (2) for different future time steps in a way as treating the underlying collision events (from which at least one has to be fulfilled) as independent. This would falsely result in $p(C_{\mathrm{V}_i,k}(T_\mathrm{P})) = 1 - \prod_{m=k}^{k+T_\mathrm{P}} (1 - p(C_m))$, which is obviously wrong as this combined probability depends on the prediction sampling rate. If, for example, two vehicles overlap (collide) for several consecutive time steps, then even if the individual collision probabilities are negligibly small, the combined probability of collision would converge to one if sampled infinitely fast due to the infinitely many product operations.

[7]As mentioned already, otherwise, a collision prediction is hardly possible as the necessary modeling of the combined traffic scene pdf would require the postulation of sensible individual drivers that try not to collide.

[8]We use 5000 trajectory samples per vehicle, a CCP of $20\,\%$, a $3\,\mathrm{s}$ prediction horizon with prediction sampling time $T = 0.1\,\mathrm{s}$. The chosen time-discretization allows the detection of collisions between two standard-sized vehicles of length $4.7\,\mathrm{m}$ up to a relative velocity of $340\,\frac{\mathrm{km}}{\mathrm{h}}$ or collisions with a point object up to a velocity of $170\,\frac{\mathrm{km}}{\mathrm{h}}$. The criticality assessment itself is performed every $300\,\mathrm{ms}$.

[9]Only mean predicted trajectories over the lane change event are shown for clarity. Combined collision probabilities are only visualized, if exceeding $5\,\%$. Deterministic CTRA and CV predictions only allow binary collision decisions (yes: $100\,\%$; no: not shown) as they do not consider uncertainty.

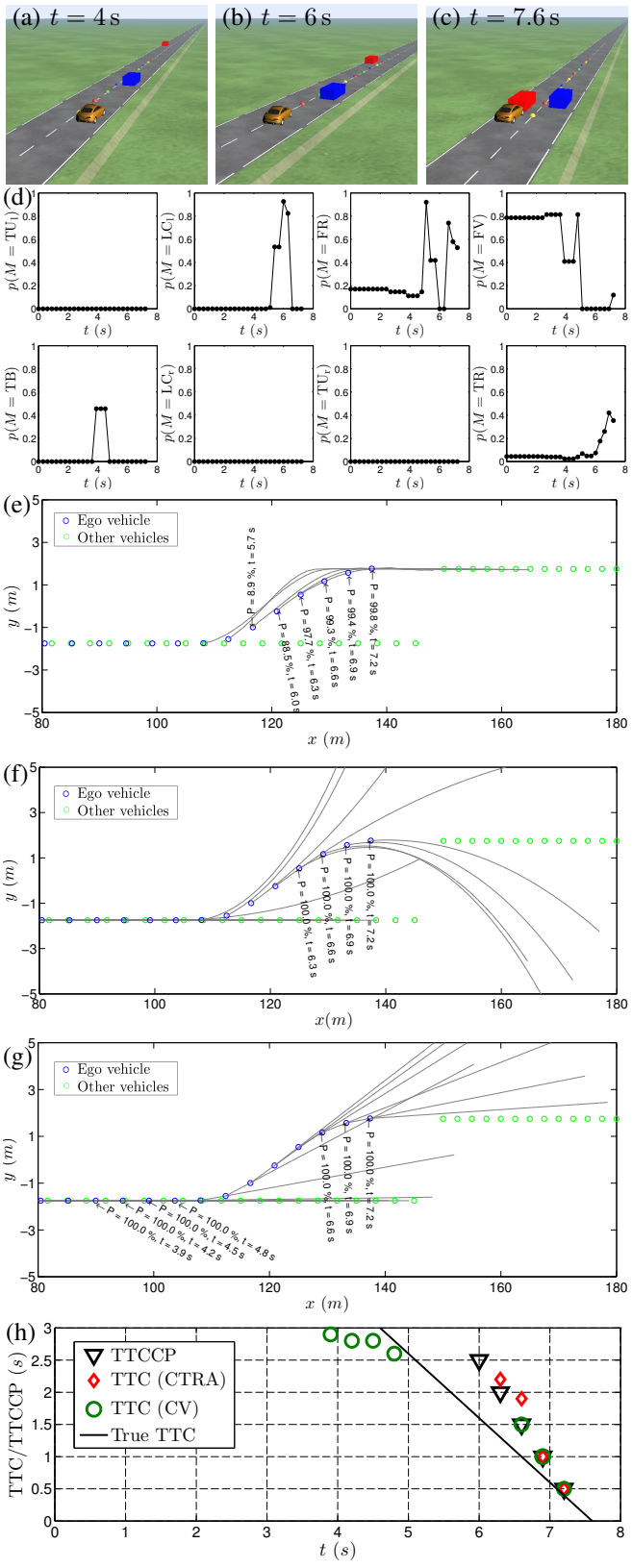

Fig. 4. Lane change scenario and collision with oncoming vehicle. Traffic scene (a,b,c); maneuver probabilities (d); bird's eye view (e,f,g) with corresponding combined collision probability for 3 s prediction horizon (e); TTC/TTCCP evolution (h).

from another false collision detection of the ego vehicle with the blue vehicle on the same lane as the predicted trajectories with high turn rate cross the original road again – a clearly non-reasonable prediction. With this in mind, our prediction approach is able to generate the criticality measure $0.9\,\mathrm{s}$ earlier than the CTRA model and $0.6\,\mathrm{s}$ earlier than a CV model. This allows timelier driver warnings – $1.6\,\mathrm{s}$ before the immanent collision in this scenario. Note that the true TTC progression as an optimal result is impossible to match for any prediction method here as, for example, $3\,\mathrm{s}$ in advance (at $t = 4.6\,\mathrm{s}$), absolutely no evidence is available that would imply an impending lane change. Our approach, however, clearly converges to the true collision time $t = 7.6\,\mathrm{s}$, the closer we reach this point in time.[10]

The second scenario is visualized in Fig. 5(a,b,c). The ego vehicle approaches an intersection while another crossing vehicle (red) approaches from the left. The ego vehicle turns to the left and finally collides with constant velocity with a standing obstacle. We first notice in Fig. 5g that the TTC for both the CTRA and CV model do not give any clue about the dangerous situation, in which both vehicles approach the intersection and can therefore not be used to warn the driver or trigger interventions. This is because the vehicles do not exactly, but only almost collide. The TTCCP value, in opposition, clearly shows the danger several seconds ($3\,\mathrm{s}$) in advance by predicting both vehicles (mainly) according to a follow road model in which the future acceleration realizations are considered uncertain. Consequently, a noticeable, non-zero combined collision probability exists as can also be seen in the bird's eye view in Fig. 5e – reflecting the criticality.[11] As soon as it becomes evident that probably no collision occurs, the TTCCP vanishes (rises to ∞) at $t = 9.6\,\mathrm{s}$. The ego vehicle then performs the turn to the left at $t \approx 10\,\mathrm{s}$, which is correctly identified via the Bayesian network, before it again follows the road, see Fig. 5d. The peak within the trash maneuver class after the turning stems from the vehicle's motion further to the right than necessary to follow the road, so that this could also mean that the driver accidentally leaves the road. After the turning, the ego vehicle collides with the standing obstacle with constant velocity at $t = 17.5\,\mathrm{s}$. In this unambiguous case, the TTCCP coincides with the TTC.

V. CONCLUSION

A novel method for long-term trajectory prediction and criticality assessment has been presented that combines a Bayesian maneuver detection with maneuver-specific, uncertain trajectory predictions to calculate the criticality measure

[10]The deviations between TTCCP and true TTC before the collision event stem from a difference between the lane change prediction model and the true, executed lane change trajectory.

[11]Eventual alarms triggered by the low TTCCP values at $t \approx 9\,\mathrm{s}$ should not be considered false alarms as all available knowledge at this point in time implies a critical situation that is only resolved when the situation evolves further. Fig. 5f additionally shows the combined collision probability as a function of the prediction length $T_\mathrm{P} \cdot T$ (in seconds) at two specific times ($t = 8.4\,\mathrm{s}$; $t = 15.3\,\mathrm{s}$) to explain how the corresponding TTCCP values emerge.

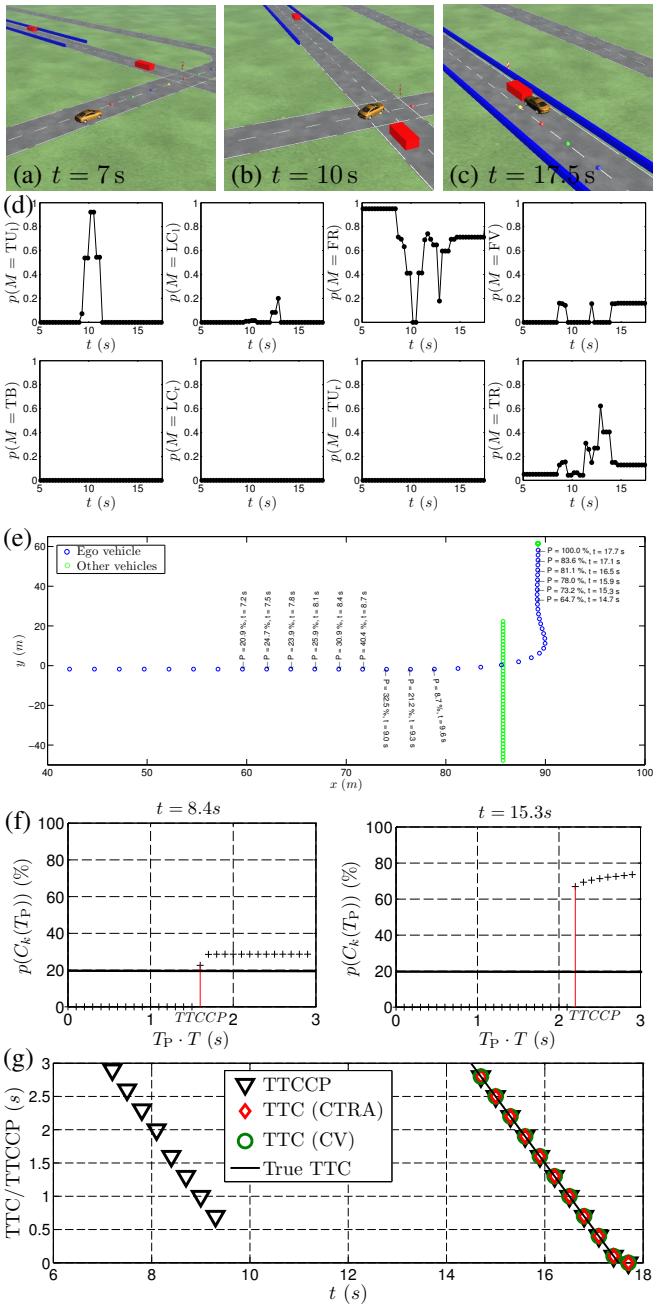

Fig. 5. Turning scenario (a) with near-collision with cross-traffic (b) and subsequent collision with stationary vehicle (c). Maneuver probabilities (d); bird's eye view with corresponding combined collision probability for 3 s prediction horizon (e); combined collision probabilities over prediction horizon length (f); TTC/TTCCP evolution (g).

TTCCP. The approach allows the suppression of false warnings, the generation of timelier true warnings in comparison to TTC as well as the generation of warnings in critical almost-collision situations, in which the TTC does not even exist. Although the approach contains novelties in the areas of maneuver detection, trajectory prediction and criticality assessment, the main contribution might lie in the throughout design of the individual components with the aim of long-term criticality assessment in mind.

ACKNOWLEDGMENTS

We kindly thank Continental for cooperation and funding within the PRORETA 3 project, which aims at the development of future concepts for integrated driver assistance systems. We further thank Igor Achieser, Yuanwen Qin, Julien Seitz and Gerrit Wege for the numerous fruitful discussions and their help in implementing the concept.

REFERENCES

[1] C. Hermes, C. Wöhler, K. Schenk *et al.*, "Long-Term Vehicle Motion Prediction," in *Proc. of the IEEE Intelligent Vehicles Symposium*, Xi'an, China, Jun. 2009, pp. 652–657.

[2] D. Vasquez and T. Fraichard, "Motion Prediction for Moving Objects: A Statistical Approach," in *Proc. of the IEEE International Conference on Robotics and Automation*, vol. 4, New Orleans, LA, USA, Apr. 2004, pp. 3931–3936.

[3] M. Althoff, O. Stursberg, and M. Buss, "Model-Based Probabilistic Collision Detection in Autonomous Driving," *IEEE Transactions on Intelligent Transportation Systems*, vol. 10, no. 2, pp. 299–310, Jun. 2009.

[4] A. Broadhurst, S. Baker, and T. Kanade, "Monte Carlo Road Safety Reasoning," in *Proc. of the IEEE Intelligent Vehicles Symposium*, Las Vegas, NV, USA, Jun. 2005, pp. 319–324.

[5] A. Eidehall and L. Petersson, "Statistical Thread Assessment for General Road Scenes Using Monte Carlo Sampling," *IEEE Transactions on Intelligent Transportation Systems*, vol. 9, no. 1, pp. 137–147, Mar. 2008.

[6] A. Lawitzky, D. Althoff, C. F. Passenberg *et al.*, "Interactive Scene Prediction for Automotive Applications," in *Proc. of the IEEE Intelligent Vehicles Symposium*, Gold Coast, Australia, Jun. 2013, pp. 1028–1033.

[7] T. Hülnhagen, I. Dengler, A. Tamke *et al.*, "Maneuver Recognition Using Probabilistic Finite-State Machines and Fuzzy Logic," in *Proc. of the IEEE Intelligent Vehicles Symposium*, San Diego, CA, USA, Jun. 2010, pp. 65–70.

[8] D. Kasper, G. Weidl, T. Dang *et al.*, "Object-Oriented Bayesian Network for Detection of Lane Change Maneuvers," *IEEE Intelligent Transportation Systems Magazine*, vol. 4, no. 1, pp. 1–10, Jan. 2012.

[9] I. Dagli, M. Brost, and G. Breuel, "Action Recognition and Prediction for Driver Assistance Systems Using Dynamic Belief Networks," *Lecture Notes in Computer Science*, vol. 2592, pp. 179–194, 2003.

[10] D. Meyer-Delius, C. Plagemann, and W. Burgard, "Probabilistic Situation Recognition for Vehicular Traffic Scenes," in *Proc. of the IEEE International Conference on Robotics and Automation*, Kobe, Japan, May 2009, pp. 459–464.

[11] M. Tsogas, X. Dai, G. Thomaidis *et al.*, "Detection of Maneuvers Using Evidence Theory," in *Proc. of the IEEE Intelligent Vehicles Symposium*, Eindhoven, The Netherlands, Jun. 2008, pp. 126–131.

[12] S. Bonnin, T. H. Weisswange, F. Kummert *et al.*, "Accurate Behavior Prediction on Highways Based on a Systematic Combination of Classifiers," in *Proc. of the IEEE Intelligent Vehicles Symposium*, Gold Coast, Australia, Jun. 2013, pp. 242–249.

[13] C. Laugier, I. E. Paromtchik, M. Perrollaz *et al.*, "Probabilistic Analysis of Dynamic Scenes and Collision Risks Assessment to Improve Driving Safety," *IEEE Intelligent Transportation Systems Magazine*, vol. 3, no. 4, pp. 4–19, 2011.

[14] J. Hillenbrand, A. M. Spieker, and K. Kroschel, "A Multilevel Collision Mitigation Approach – Its Situation Assessment, Decision Making, and Performance Tradeoffs," *IEEE Transactions on Intelligent Transportation Systems*, vol. 7, no. 4, pp. 528–540, Dec. 2006.

[15] A. Berthelot, A. Tamke, T. Dang *et al.*, "Stochastic Situation Assessment in Advanced Driver Assistance System for Complex Multi-Objects Traffic Situations," in *Proc. of the IEEE/RSJ International Conference on Intelligent Robots and Systems*, Vilamoura, Algarve, Portugal, Oct. 2012, pp. 1180–1185.

[16] J. Schneider, A. Wilde, and K. Naab, "Probabilistic Approach for Modeling and Identifying Driving Situations," in *IEEE Intelligent Vehicles Symposium*, Eindhoven, The Netherlands, Jun. 2008, pp. 343–348.

[17] N. E. Du Toit and J. W. Burdich, "Probabilistic Collision Checking With Chance Constraints," *IEEE Transactions on Robotics*, vol. 27, no. 4, pp. 809–815, Aug. 2011.